THE JOURNAL OF PHYSICAL CHEMISTRY B

ARTICLE

pubs.acs.org/JPCB

Experimental and Theoretical Study of the Vibrational Spectra of Oligoureas: Helical versus β-Sheet-Type Secondary Structures

Dominique Cavagnat,[†] Paul Claudon,[‡] Lucile Fischer,[‡] Gilles Guichard,[‡] and Bernard Desbat*[,‡]

[†]ISM, UMR CNRS 5255, Université Bordeaux, 351 cours de la libération, 33405 Talence, France

[‡]CBMN, UMR CNRS 5248, Université Bordeaux, ENITAB, Institut Européen de Chimie et Biologie (IECB), 2 rue Robert Escarpit, 33607 Pessac, France

Supporting Information

ABSTRACT: Ab initio calculations of two oligoureas stabilized in helix and sheet organization have been performed. The hydrogen bond distances were found to be almost the same for both structures. The vibrational assignment of the two oligourea structures and the direction of the transition moment of each vibration have been determined. From these results, and using the experimental isotropic optical index determined for one oligourea, we have established the anisotropic infrared optical files for the two structures. Interestingly, most urea absorptions vibrate in only one principal direction. Also, the shift of the carbonyl band is weaker and inverse to what was reported for corresponding protein secondary structures. Finally, simulations of the Polarization Modulation Infrared Reflection Absorption Spectroscopy (PMIRRAS) and Attenuated Reflection Spectroscopy (ATR) infrared spectra demonstrate the possibility to determine the orientation of the oligoureas in thin or ultrathin films, even if in some cases it may be difficult to unambiguously assign their secondary structure.

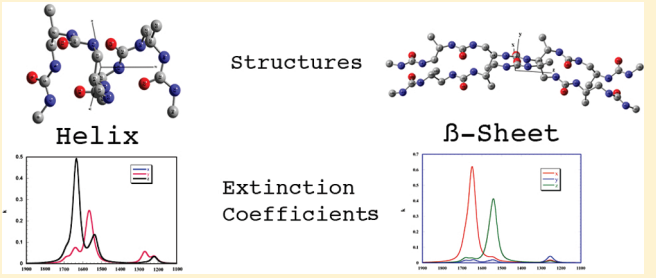

INTRODUCTION

In the field of peptidomimetics, aliphatic oligomers consisting of N,N′-linked urea bridging units are receiving increasing attention.[1] This interest stems from the diversity of available side-chain appendages, resistance to protease degradation, and the high folding propensity of these oligomers. Recently reported biological applications include the design of host-defense peptide mimetics as antimicrobial agents.[2,3] The backbone of these oligomers is similar to that of γ-peptides because the periodic pattern of the γ-peptides, $-CH_2CONHCHRCH_2-$, is replaced by the pattern $-NHCONHCHRCH_2-$. The oligoureas have been shown to form a stable 2.5 helical structure, reminiscent of the 2.6_{14} helical structure of γ-peptides.[4] This helical secondary structure is largely stabilized by the aptitude of the urea group to form three-centered hydrogen bonds.

In the case of α-peptides, it is well-known that the most intense vibrational mode (Amide I) is sensitive to secondary structure.[5,6] On the contrary, the link between oligourea secondary structure and vibrational frequency modes has never been established. Similarly, the directions of the transition moments of the most intense modes of the oligoureas with respect to their molecular axes of symmetry are not known, preventing any orientational analysis of these compounds from their vibrational spectra.

Thus, we have performed ab initio calculations of the vibrational modes of an oligourea stabilized in two secondary structures: helix and β-sheet organizations, to assign experimental spectra and identify the directions of the transition moments of the most intense vibrations. Moreover, the infrared anisotropic optical indices of both secondary structures have been generated from the transition values to simulate the Polarization Modulation Infrared Reflection Absorption Spectroscopy (PMIRRAS) and Attenuated Reflection Spectroscopy (ATR) spectra with respect to the orientation of the secondary structure.

EXPERIMENTAL PROCEDURES

Synthesis. The synthesis of the urea-octamer **1** as a trifluoroacetate salt (Chart 1) has been previously reported.[3] Oligourea **1** was previously found to display strong helix propensity and to exhibit significant antibacterial activity by disrupting bacterial membranes.

Infrared Spectra. The ATR spectra were recorded using a Nexus 6700 Nicolet at 4 cm^{-1} resolution using a Miracle cell (Spyke technology) equipped with a single reflection germanium crystal.

Ab Initio Calculations and Simulation of PMIRRAS and ATR Spectra. To reduce calculation time, the number of atoms was minimized, and the calculations were performed with heptaurea **2** and a noncovalent dimer of pentaurea **3** (namely,

Received: November 17, 2010
Revised: March 2, 2011
Published: March 29, 2011

Chart 1

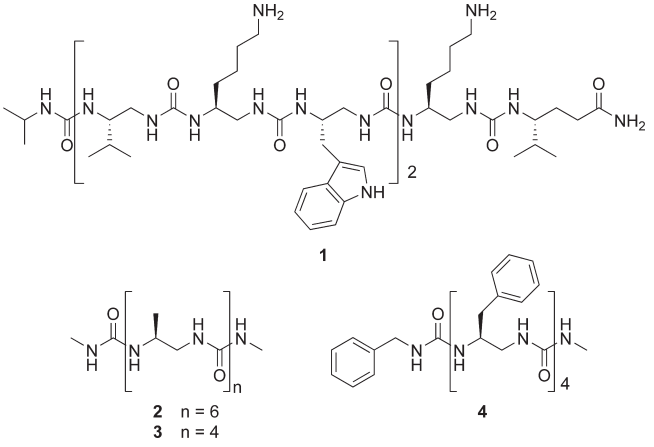

3·3) bearing Ala side chains and terminal methyl chains, for the helix and β-sheet-type structure, respectively.

The starting geometry of the helix structure of **2** was determined from the atomic positions of the helix in the crystalline structure of related oligourea **4**.[7] With the help of the Chem3D software, a β-sheet-type structure was obtained by unfolding the helix to get a linear conformation, and then the chain was doubled to form **3·3**. The energy was minimized, and the atomic positions were then introduced in the ab initio software.

The geometry optimizations, vibrational frequencies, and absorption intensities of both **2** and **3·3** were calculated by the Gaussian 09 program[8] using four processors on an SGI IRIX64.

At first, calculations were performed at the density functional theory level using B3PW91, a functional often successfully used for molecules containing N and O atoms. Owing to the large number of atoms in this system (104 and 148 atoms for the helix and β-sheet structures, respectively), only a relatively small basis set 6-31G* was tried (giving rise to 832 and 1180 basis functions, 1568 and 2224 Gaussian primitives for the helix and β-sheet structures, respectively). To better describe the hydrogen bond, a polarization function p was then included (6-31G** giving rise to 1000 and 1420 basis functions and 1736 and 2464 Gaussian primitives for the helix and β-sheet structures, respectively). Finally, we have used the new wB97DX functional[9] with the 6-31G** basis set. This new functional provides significant improvement for nonbonded interactions and can thus be more appropriate for calculations implying hydrogen bonds.

For comparison to experimental data, the calculated frequencies were scaled by a factor of 0.941 (B3PW91/6-31G**) or 0.929 (wB97DX/6-31G**), except for the urea II bands which were scaled by a factor of 0.965 and 0.953. This difference in the relative frequency position is equivalent to the difference reported for the amide I and amide II bands given by the ab initio calculation of peptide systems.[10]

The x, y, and z components of the dipole moments corresponding to each vibration were calculated from the ab initio computed atomic polar tensors and do not change significantly with the various calculations.[8]

Homemade software named *Multicouche*[11] was used to obtain the optical indexes of the helix and β-sheet oligoureas and to simulate both their PMIRRAS spectra on a water monolayer surface and their polarized ATR spectra. The experimental s polarized ATR IR spectrum of **1** in powder form has been recorded on a germanium crystal and used to calculate the complex isotropic indexes of oligoureas. Finally, we have established both anisotropic optic files for the oligourea structures in the infrared region, assuming for both secondary structures that the isotropic absorption index (k) is related to the uniaxial anisotropic indexes by the expression $k = (k_x + k_y + k_z)/3$, with $k_x = k_y$, and taking into account the ratio intensity (k_z/k_x) of the main absorption bands given by the ab initio calculations.

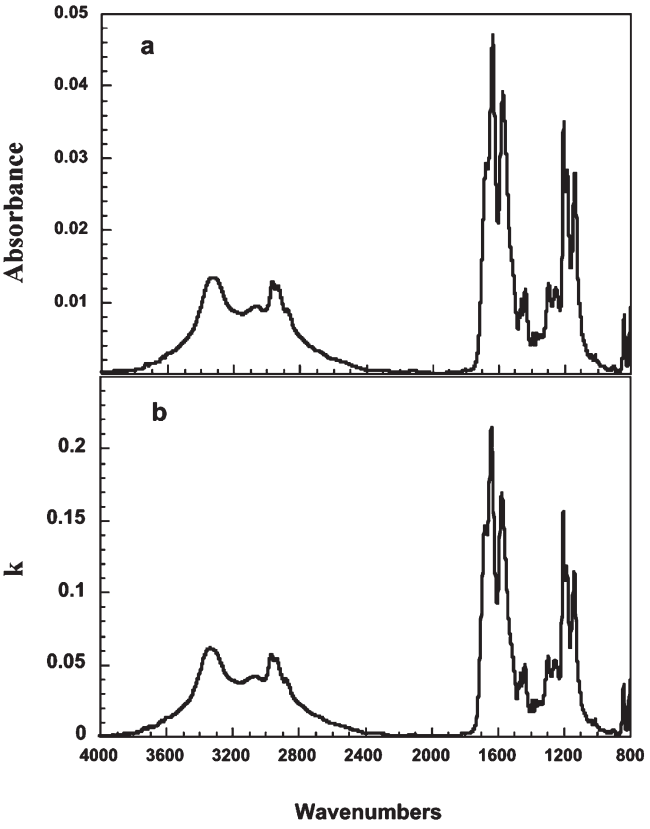

Figure 1. (a) s polarized ATR infrared spectrum of **1** as a powder. (b) Isotropic extinction coefficient k of compound **1**.

RESULTS

First, we determined the optical indices of the isotropic compound **1** in the infrared region. Figure 1a displays the s polarized ATR spectrum (germanium crystal) of **1** in powder form. The spectrum was dominated by two strong bands centered at 1633 and 1571 cm^{-1} similar to the amide I and amide II bands of the α-polypeptide chain in peptides and proteins. This is essentially due to carbonyl stretching and the coupled CN stretching NH deformation, respectively. Hereafter, these two vibrations will be referred to as "urea I" and "urea II", respectively.

Using the *Multicouche* software developed by our group,[11] we have calculated the complex optical index $\tilde{n}$ ($\tilde{n} = n + ik$), as seen in Figure 1b, which best reproduces the experimental ATR spectrum of **1**. The k_{max} (~0.22) of the strong urea I band at 1633 cm^{-1} is weaker than the average value of a protein amide I band ($k_{max} \sim 0.35$). This is probably because the carbonyl density of the repeating pattern of the urea group is weaker than in the case of the amide group in α-polypeptide chains.

dx.doi.org/10.1021/jp1109674 |J. Phys. Chem. B 2011, 115, 4446–4452

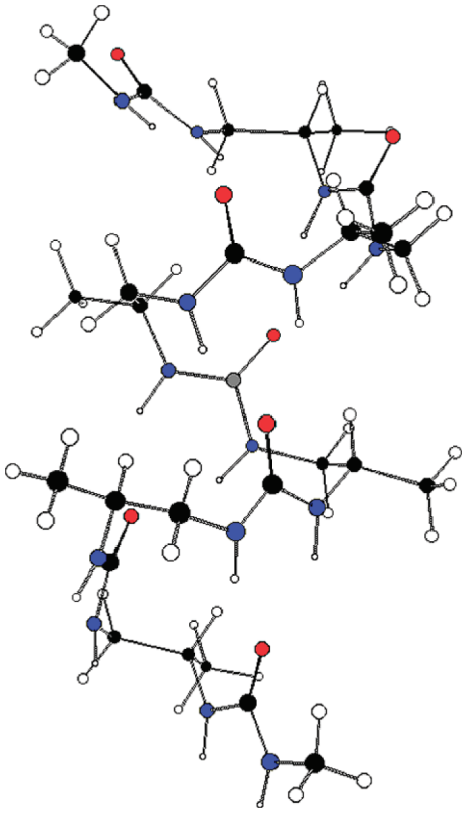

Figure 2. Representation of the optimized helix structure for oligourea **2**. Black, carbon; white, hydrogen; blue, nitrogen; red, oxygen.

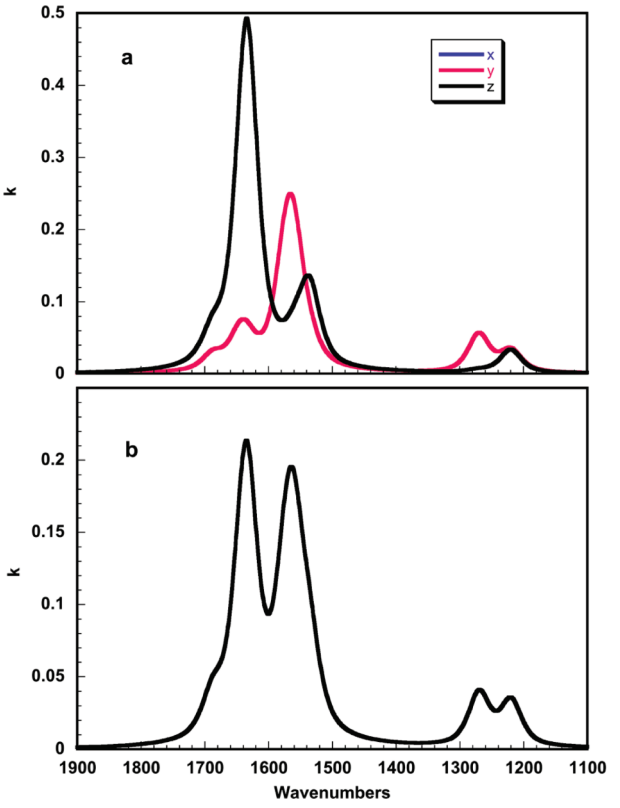

Figure 3. (a) Calculated k anisotropic extinction coefficient of helix oligourea **2**. (b) Calculated k isotropic extinction coefficient of helix oligourea **2**.

Calculation of the Helix Structure. The helix structure of **2** obtained after ab initio calculation is presented Figure 2 (Supporting Information S1). The z direction was assigned to the principal axis of the helix, with the (x, y) plane perpendicular to the helix axis. The hydrogen bond distances between the oxygen and corresponding nitrogen atoms were consistently around 2.97 Å, which is very close to the average distance reported for the α helix in proteins (2.99 Å).[12] Moreover, both hydrogen bonds on each oxygen atom have almost similar value (2.92/3.02 Å), which increases the stability of the oligourea structure in comparison to the α helix of peptides which is stabilized by only one hydrogen bond.

The vibrational ab initio calculations provided the contribution of the transition moment of each mode along the three principal directions of the helix (Supporting Information S2). Taking into account these results and the experimental isotropic indices, we built an anisotropic optical index file characteristic of the oligourea 2.5-helix structure. We used only the most intense bands to create the final optical index file (Figure 3a). It is clear that the strongest absorption (urea I) near 1630 cm^{-1} is essentially directed along the helix axis because its dichroïc ratio (k_z/k_x) is equal to 6.51. This ratio value is greater than the value observed for the amide I band in the case of the α helix (2.27). The region near 1565 cm^{-1} is more complex because the urea II band contains two components, a strong one at 1565 cm^{-1} and a smaller one at 1536 cm^{-1}. The first component is almost completely polarized and degenerated in the (x, y) plane, whereas the second component is polarized along the z direction. The splitting of this mode in two components reveals the coupling of the two ν CN + NH deformations of the urea group with two vibrational components in phase and out of phase.

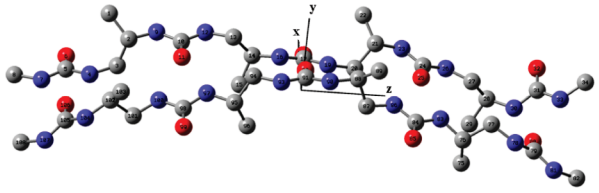

Figure 4. Optimized geometry of the oligourea β-sheet **3**·**3**.

This polarization effect on urea II differs from the effect observed for amide II in the α helix structure, where the vibration has only a very small component along the z direction. The indices present also one smaller band around 1250 cm^{-1} (urea III) equivalent to the amide III band observed from proteins. Finally, the isotropic optical indices (Figure 3b), calculated with the anisotropic indices ($k = (k_x + k_y + k_z)/3$) reproduce well the experimental indices (Figure 1b). The main differences were simply due to the presence of trifluoroacetate bands (1675, 1230, and 1150 cm^{-1}) on the spectrum of **1**.

Calculation of the β-Sheet-Type Structure. Although the oligourea β-sheet-like structure has never been observed experimentally, the ab initio calculation shows that the final geometry of the β structure displayed in Figure 4 (Supporting Information S3) is a slightly curved plane with the urea chains along the z direction and the carbonyl bonds parallel to the x direction.

The y direction is more or less perpendicular to the plane of the β-sheet. Most of the hydrogen bonds are similar, with average distances (N···O) equal to 2.93 Å, a value that is almost the same as that obtained for the 2.5-helical structure. However, this

dx.doi.org/10.1021/jp1109674 |J. Phys. Chem. B 2011, 115, 4446–4452

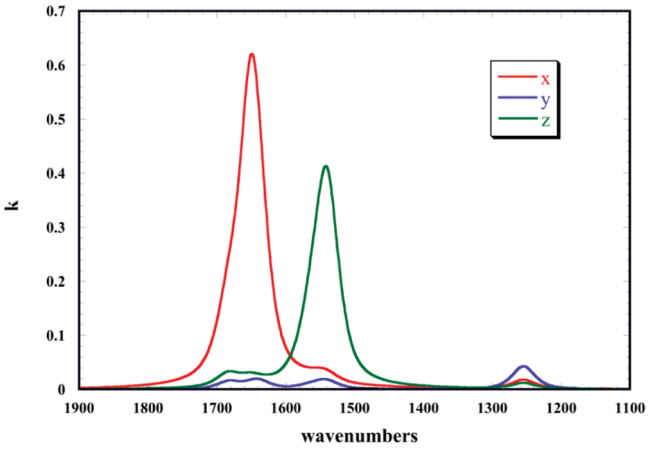

Figure 5. Anisotropic extinction coefficient of the oligourea β-sheet structure **3·3**.

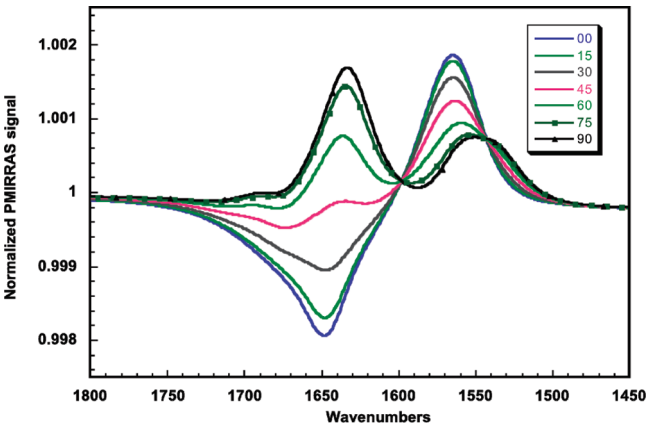

Figure 6. PMIRRAS spectra of the helix oligourea monolayer on water versus the tilt angle.

distance is similar to the average distance (2.94 Å) found in the protein β-sheet (parallel or antiparallel).[12] Using the same procedure for the helix structure, an anisotropic file associated with β-sheet conformation was built from the direction of the transition moment of each vibration. The optical anisotropic file is presented Figure 5 (Supporting Information S4).

The data show that the principal bands of this structure are strongly polarized. Indeed, the urea I possesses a dichroïc ratio of 20 and the urea II a dichroïc ratio of 0.05. These vibrations can be considered to be purely in the x and z directions, respectively. The position of the β-sheet urea I vibration was calculated to be at 1649 cm^{-1}, a value higher than that obtained for the 2.5-helical structure (1630 cm^{-1}, vide supra) contrary to the red shift observed in the case of proteins. Moreover, the absolute shift between the two structures (19 cm^{-1}) is significantly lower than in the case of proteins (~35 cm^{-1}). This weaker splitting should be related to the greater distance between the carbonyl groups in the oligourea compound, producing a decrease of the dipole−dipole interaction and consequently a decrease of the vibrational coupling. The urea II vibration situated at 1542 cm^{-1}, equivalent to the amide II band, was almost single, and significantly, at lower frequency than the similar band observed for the oligourea helix structure. In summary, the shifts in frequencies in relation to structure were smaller for the oligoureas compared to the

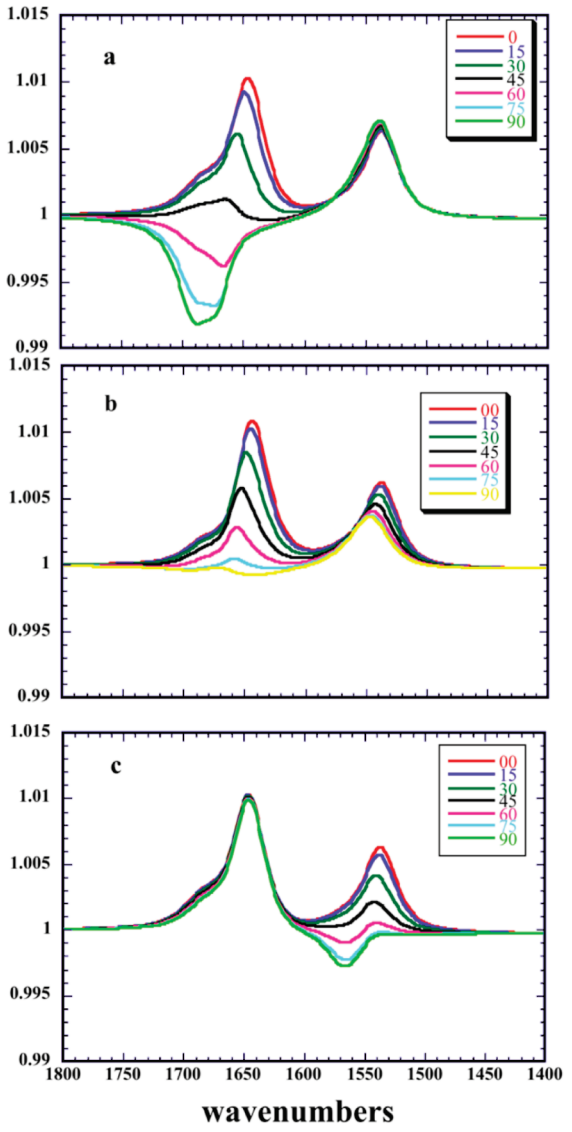

Figure 7. Simulation of PMIRRAS spectra of β-sheet oligourea **3·3** on water versus the tilt angle θ, with Ψ angles of (a) 0°, (b) 45°, and (c) 90°.

α-peptide systems, thus making the determination of their secondary structures from their infrared spectra more difficult.

Expected PMIRRAS and ATR Spectra for the Two Structures with Respect to Their Orientation. The simulated PMIRRAS spectra of the oriented oligourea helix on the water surface are represented in Figure 6. The general profile of the spectra is similar to that of the spectra obtained for the α-helix under the same conditions.[13] For example, the urea I frequency appears at a higher value when the helix is vertical than when the helix is flat at the surface (LO−TO splitting). However, the spectra of helical oligoureas and α-peptides present some distinct features. For example, the urea I is mainly polarized along only one direction, while the urea II is polarized along all three directions in space.

The simulations show that the main modifications appear on the urea II band shape, which changes with the oligourea orientation. This presents two distinct components when the helix is tilted by more than 45° with respect to normal at the interface.

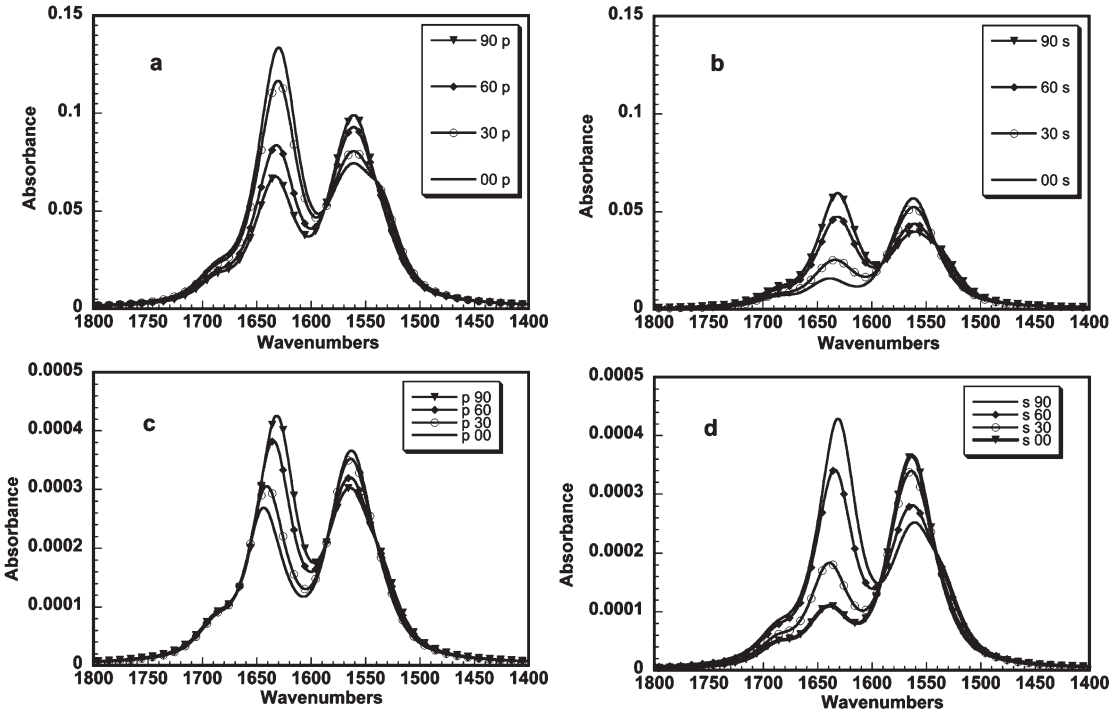

Figure 8. Simulation of the ATR spectra of thin (a,b) and ultrathin (c,d) films versus the tilt angle of the oligourea helix.

Table 1. ATR Dichroïc Ratio Calculated for the Urea I and Urea II Vibrations of the Oligourea Helix in Thin and Ultrathin Film

thickness	3 μm		15 Å	
θ	urea 1	urea 2	urea 1	urea 2
0°	8.85	1.3	2.16	0.986
15°	7.16	1.367	1.95	1.006
30	4.58	1.533	1.562	1.041
45°	2.8	1.791	1.277	1.097
60°	1.75	2.121	1.12	1.18
75°	1.3	2.3	1.027	1.263
90°	1.11	2.49	0.993	1.305

Table 2. ATR Dichroïc Ratio of the Urea I and Urea II Bands in 3 μm Thin Films at Three Ψ Angles (0°, 45°, 90°) and Four θ Angles (0°, 30°, 60°, 90°) of the β-Sheet Orientations

ψ	0°		45°		90°	
θ	urea 1	urea 2	urea 1	urea 2	urea 1	urea 2
0°	0.966	0.819	18.3	0.128	0.966	0.819
30°	1.782	0.907	12.2	0.313	0.935	1.485
60°	7.195	1.071	9.57	1.080	0.895	5.465
90°	29.90	1.14	3.07	3.233	0.885	17.46

The simulated PMIRRAS spectra of the β-sheet oligourea on water surface are presented in Figures 7a−c. The number of simulations is more important because the β-sheet structure does not present a revolution axis, and the calculation should be done with two Euler angles. The first angle was defined by the tilt angle θ of the oligourea chains with respect to the normal plane, and the second angle Ψ is the rotation of the β plane around the axis of the oligourea chains. To limit the number of graphics, only three Ψ angles were presented (0°, 45°, and 90°). The various simulations show that multiple spectral shapes can be observed depending on the orientation of the β-sheet.

However, the spectra can be easily interpreted because the two principal bands have nearly aligned transition moments with the axes of the β-sheet plane. Therefore, the selection rule of the PMIRRAS on dielectrics for one single vibration can be applied.[14] We expect one strong positive band when its transition moment is in the plane of the interface, a negative medium band when its transition moment is perpendicular to the interface, and disappearance of the band when the transition moment is at the magic angle with respect to the normal plane (38° for water).

The polarized infrared ATR method is also a technique largely employed to get information on the interaction of peptides or proteins with organized lipid multilayers.[15,16] For this reason, we have performed the ATR simulations of ultrathin film and bulk film for both secondary structures represented by the oligoureas **2** and **3·3**. We present in Figure 8 the simulation of the ATR spectra of the helix oligourea versus its tilt angle.

A defining characteristic observed in the analysis of the α-helix structure of **2** is the variation of the shape of the urea II band with respect to the tilt angle, which is likely due to the presence of two opposite polarization components. However, this effect is less pronounced in the PMIRRAS spectra. Another effect, which is worth mentioning, is the significant shift at high frequency of the urea I band for the small tilt angles in the case of the ultrathin film system. In Table 1, the dichroïc ratios expected for the urea I and urea II vibrations are reported. The ratio variations are more evident in the thin film system than in the ultrathin film system. Therefore, the orientation determination will be more difficult for the ultrathin film. However, the variations are more evident in

dx.doi.org/10.1021/jp1109674 |J. Phys. Chem. B 2011, 115, 4446–4452

Table 3. ATR Dichroïc Ratio of the Urea I and Urea II Bands in a 15 Å Ultrathin Film at Three Ψ Angles (0°, 45°, 90°) and Four θ Angles (0°, 30°, 60°, 90°) of the β-Sheet Orientations

ψ	0°		45°		90°	
θ	urea 1	urea 2	urea 1	urea 2	urea 1	urea 2
0°	0.941	0.952	23.99	0.096	0.947	0.951
30°	1.081	0.955	18.64	0.137	0.949	1.073
60°	1.963	0.961	6.75	0.371	0.955	1.752
90°	6.73	0.962	1.404	1.228	0.956	3.714

the case of these oligoureas compared to the previously published α-helix dichroïc ratio for proteins.[17]

Using the *Multicouche* software, we have simulated the ATR spectra of thin and ultrathin films of the β-sheet oligourea versus its orientation. The dichroïc ratio data are reported in Tables 2 and 3. The range of the dichroïc ratio variations for the 3 μm thin film is systematically larger than the range obtained with the ultrathin film, in agreement with the previously observed behavior of polarized ATR spectra on organized films. The simulations show, like for the PMIRRAS method, that some β-sheet orientations can be easily determined, while others are more difficult to discriminate because their dichroïc ratios do not present a significant variation with respect to the tilt angle. However, this problem is similar to that encountered for the orientation determination of the protein β-sheet.[17] In summary, we have assigned the directions of the transition moments of urea vibrations in the helix and β-sheet structures of oligoureas. Our calculations provide the first indication that β-sheet type structures are accessible by oligoureas. The calculated hydrogen bond distances in the model oligoureas were found to be similar between β-sheet and helical structures. This is in contrast to the case of proteins, where a clear decrease in the hydrogen bond distance is observed in the β-sheet structure. The urea I frequency shift between the two structures is weaker than and inverse of the amide I shift observed in protein secondary structures. The determination of the structure of an oligourea based on its infrared spectrum will be more difficult than for a polypeptide chain, even if the frequency shift of the urea II is larger than that of the amide II vibration. Although simulated PMIRRAS and ATR spectra of oligoureas and α-polypeptides share an overall similarity, the shape of the urea II band with respect to the orientation of the oligourea helix was found to differ significantly compared to that of the amide II band. The theoretical and experimental data reported herein will be of practical use for further analysis of PMIRRAS and ATR spectra of oligoureas, for example, the interaction of antimicrobial oligoureas with phospholipids membranes.[2,3]

■ ASSOCIATED CONTENT

Supporting Information. S1: Atom positions in the final stabilized helix structure **2** obtained from ab initio calculations. S2: Helix structure **2**, frequencies, and directions of the transition moment obtained from ab initio calculations. S3: Atom positions in the final stabilized β-sheet structure **3·3** obtained from ab initio calculations. S4: β-sheet structure **3·3**, frequencies, and directions of the transition moment obtained from ab initio calculations.

This material is available free of charge via the Internet at http://pubs.acs.org.

■ AUTHOR INFORMATION

Corresponding Author

*Phone: 33 5 40 00 30 46. Fax: 33 5 40 00 30 73. E-mail: b.desbat@cbmn.u-bordeaux.fr.

■ ACKNOWLEDGMENT

The authors acknowledge computational facilities provided by the Pôle Modélisation of the Institut des Sciences Moléculaires (University Bordeaux 1). This work was supported in part by the Centre National de la Recherche Scientifique (CNRS), the Region Aquitaine, the University of Bordeaux, and by a grant from the Agence Nationale de la Recherche (grant n°. ANR-07-PCVI-0018). A CIFRE fellowship from ImmuPharma France and the Association Nationale pour la Recherche Technique (ANRT) for P.C. is gratefully acknowledged.

■ REFERENCES

(1) Fischer, L.; Guichard, G. *Org. Biomol. Chem.* **2010**, *8*, 3101–3117.
(2) Violette, A.; Fournel, S.; Lamour, K.; Chaloin, O.; Frisch, B.; Briand, J. P.; Monteil, H.; Guichard, G. *Chem. Biol.* **2006**, *13*, 531–538.
(3) Claudon, P.; Violette, A.; Lamour, K.; Decossas, M.; Fournel, S.; Heurtault, B.; Godet, J.; Mély, Y.; Jamart-Gregoire, B.; Averlant-Petit, M. C.; Briand, J. P.; Duportail, G.; Monteil, H.; Guichard, G. *Angew. Chem., Int. Ed.* **2010**, *49*, 333–336.
(4) Violette, A.; Averlant-Petit, M. C.; Semetey, V.; Hemmerlin, C.; Casimir, R.; Graff, R.; Marraud, M.; Briand, J. P.; Rognan, D.; Guichard, G. *J. Am. Chem. Soc.* **2005**, *127*, 2156–2164.
(5) Miyazawa, T. *Infrared Spectra and Helical Conformations in Poly-α-Amino Acids*; Marcel Dekker: New York, 1967.
(6) Goormaghtigh, E.; Cabiaux, V.; Ruysschaert, J. M. *Subcell. Biochem.* **1994**, *23*, 405–450.
(7) Fischer, L.; Claudon, P.; Pendem, N.; Miclet, E.; Didierjean, C.; Ennifar, E.; Guichard, G. *Angew. Chem., Int. Ed. Engl.* **2010**, *49*, 1067–70.
(8) Frisch, M. J.; Trucks, G. W.; Schlegel, H. B.; Scuseria, G. E.; Robb, M. A.; Cheeseman, J. R.; Scalmani, G.; Barone, V.; Mennucci, B.; Petersson, G. A.; Nakatsuji, H.; Caricato, M.; Li, X.; Hratchian, H. P.; Izmaylov, A. F.; Bloino, J.; Zheng, G.; Sonnenberg, J. L.; Hada, M.; Ehara, M.; Toyota, K.; Fukuda, R.; Hasegawa, J.; Ishida, M.; Nakajima, T.; Honda, Y.; Kitao, O.; Nakai, H.; Vreven, T.; Montgomery, J. A., Jr.; Peralta, J. E.; Ogliaro, F.; Bearpark, M.; Heyd, J. J.; Brothers, E.; Kudin, K. N.; Staroverov, V. N.; Kobayashi, R.; Normand, J.; Raghavachari, K.; Rendell, A.; Burant, J. C.; Iyengar, S. S.; Tomasi, J.; Cossi, M.; Rega, N.; Millam, N. J.; Klene, M.; Knox, J. E.; Cross, J. B.; Bakken, V.; Adamo, C.; Jaramillo, J.; Gomperts, R.; Stratmann, R. E.; Yazyev, O.; Austin, A. J.; Cammi, R.; Pomelli, C.; Ochterski, J. W.; Martin, R. L.; Morokuma, K.; Zakrzewski, V. G.; Voth, G. A.; Salvador, P.; Dannenberg, J. J.; Dapprich, S.; Daniels, A. D.; Farkas, Ö.; Foresman, J. B.; Ortiz, J. V.; Cioslowski, J.; Fox, D. J. *Gaussian 09*; Gaussian, Inc.: Wallingford CT, 2009.
(9) Chai, J.-D.; Head-Gordon, M. *Phys. Chem. Chem. Phys.* **2008**, *10*, 6615–6620.
(10) Kubelka, J.; Huang, R.; Keiderling, T. A. *J. Phys. Chem. B* **2005**, *109*, 8231–8243.
(11) Buffeteau, T.; Blaudez, D.; Péré, E.; Desbat, B. *J. Phys. Chem. B* **1999**, *103*, 5020–5027.
(12) Koch, O.; Bocola, M.; Klebe, G. *Proteins: Struct., Funct., Bioinf.* **2005**, *61*, 310–317.

(13) Blaudez, D.; Turlet, J. M.; Dufourc, J.; Bard, D.; Buffeteau, T.; Desbat, B. *J. Chem. Soc., Faraday Trans.* **1996**, *92*, 525–530.
(14) Blaudez, D.; Buffeteau, T.; Cornut, J. C.; Desbat, B.; Escafre, N.; Pezolet, M.; Turlet, J. M. *Appl. Spectrosc.* **1993**, *47*, 869–874.
(15) Frey, S.; Tamm, L. K. *Biophys. J.* **1991**, *60*, 922–930.
(16) Reiter, G.; Siam, M.; Falkenhagen, D.; Gollneritsch, W.; Baurecht, D.; Fringeli, U. P. *Langmuir* **2002**, *18*, 5761–5771.
(17) Castano, S.; Desbat, B. *Biochim. Biophys. Acta* **2005**, *1715*, 81–95.